

# Impact of Electric Fields on Highly Excited Rovibrational States of Polar Dimers

Rosario González-Férez<sup>1</sup> and Peter Schmelcher<sup>2,3</sup>

<sup>1</sup>*Instituto 'Carlos I' de Física Teórica y Computacional and Departamento de Física Atómica Molecular y Nuclear, Universidad de Granada, E-18071 Granada, Spain*

<sup>2</sup>*Theoretische Chemie, Physikalisch-Chemisches Institut, Im Neuenheimer Feld 229, D-69120 Heidelberg, Germany*

<sup>3</sup>*Physikalisches Institut, Universität Heidelberg, Philosophenweg 12, D-69120 Heidelberg, Germany\**

(Dated: August 29, 2018)

We study the effect of a strong static homogeneous electric field on the highly excited rovibrational levels of the LiCs dimer in its electronic ground state. Our full rovibrational investigation of the system includes the interaction with the field due to the permanent electric dipole moment and the polarizability of the molecule. We explore the evolution of the states next to the dissociation threshold as the field strength is increased. The rotational and vibrational dynamics are influenced by the field; effects such as orientation, angular motion hybridization and squeezing of the vibrational motion are demonstrated and analyzed. The field also induces avoided crossings causing a strong mixing of the electrically dressed rovibrational states. Importantly, we show how some of these highly excited levels can be shifted to the continuum as the field strength is increased, and reversely how two atoms in the continuum can be brought into a bound state by lowering the electric field strength.

PACS numbers: 32.60.+i,33.20.Vq,33.80.Gj

## I. INTRODUCTION

The recent availability of cold to ultracold polar dimers in the vibrational and rotational ground state of their singlet electronic ground potential [1, 2], represents a breakthrough towards the control of all molecular degrees of freedom, i.e., the center of mass, electronic, rotational and vibrational motions, and towards the ultimate goal of obtaining a polar condensate. The experimental achievements have been accompanied by significant theoretical efforts to understand the intriguing physical phenomena expected for ultracold polar quantum gases due to their anisotropic and long-range dipole-dipole interaction. In particular it has been analyzed how external fields can control and manipulate the scattering properties [3, 4, 5, 6], and the chemical reactions dynamics [7], or how to use them as tools for quantum computational devices [8, 9, 10]. Different approaches to achieve cold and ultracold molecules have been explored [11, 12, 13, 14, 15]. For further work and references we refer the reader to the comprehensive reviews [16, 17].

The most widespread techniques to produce ultracold polar molecules are the photoassociation of two ultracold atoms [18, 19], and the tuning of the atomic interactions via magnetically induced Feshbach resonances [20]. Alternative pathways explore the ability to manipulate the interaction between atoms by inducing optical Feshbach resonances. Based on the same principle as the magnetically induced Feshbach resonances, they appear when two colliding ultracold atoms are coupled to a bound state of the corresponding molecular system by using a radiation field. Initially, there were several theoretical proposals to obtain these resonances with the help of radio-frequency, static electric, and electromagnetic fields [21, 22, 23, 24]. In addition, it has been demonstrated that a combination of a magnetic and static electric field can induce Feshbach resonances in a binary mixture of Li and Cs atoms [25, 26], and that a suitable combination of these two fields can tune the relevant interaction parameters, such as the width and open-channel scattering length in these resonances [27]. The existence of this optically induced resonances has been experimentally proved for different atomic species by tuning the laser frequency near a photoassociation resonance [28, 29, 30, 31].

Within the above experimental techniques, the molecules are usually in a highly excited vibrational level close to the dissociation threshold of an electronic state. These vibrational states are exposed to external fields and most of their overall probability is located at the outermost hump of their probability density. In the present work, we investigate the few last most weakly bound states of the  $X^1\Sigma^+$  electronic ground state of a polar molecule in a strong static electric

---

\*Electronic address: rogonzal@ugr.es, Peter.Schmelcher@pci.uni-heidelberg.de

field. We perform a full rovibrational investigation of the field-dressed nuclear dynamics including the interaction of the field with the molecular electric dipole moment and polarizability. The LiCs dimer is a prototype system and will be used here. This choice is based on the experimental interest in this system and the availability of its molecular polarizabilities [32]. It completes our previous investigations on the effects of an electric field on this system, where we have analyzed the rovibrational spectrum, the radiative decay properties, and the formation of these ultracold dimers via single-photon photoassociation from the continuum into its electronic ground state [13, 14, 33, 34, 35]. Specifically, we analyze the binding energies and the expectation values,  $\langle \cos \theta \rangle$ ,  $\langle \mathbf{J}^2 \rangle$  and  $\langle R \rangle$ , of states lying in the spectral region with binding energies smaller than  $0.28 \text{ cm}^{-1}$  and vanishing azimuthal quantum number in the very strong field regime. We demonstrate that both the rotational and vibrational dynamics are significantly affected by the field. Indeed, the vibrational motion is squeezed or stretched to minimize the energy, depending on the rotational degree of excitation and the field strength. At such strong fields the nuclear spectrum exhibits several avoided crossings between energetically adjacent states, which lead to a strongly distorted rovibrational dynamics. The latter might be directly observable when imaged by photodissociation experiments. Beyond this, (magnetically induced) avoided crossings in  $\text{Cs}_2$  have been used to construct a molecular Stückelberg interferometer [36]. In addition, we show that by tuning the electric field strength a dissociation channel is opened, i.e., a weakly bound molecular state with low-field seeking character is shifted to the atomic continuum by increasing the field strength. Of course, the reverse process is also possible, and two free atoms can be brought into a molecular bound state by lowering the field strength. This might be of interest to control the collisional dynamics of the atomic/molecular cold gas by using either very strong static (micro-) electric fields or strong quasistatic, i.e., time-dependent fields.

## II. THE ROVIBRATIONAL HAMILTONIAN

We consider a heteronuclear diatomic molecule in its  $^1\Sigma^+$  electronic ground state exposed to a homogeneous and static electric field. Our study is restricted to a non-relativistic treatment and addresses exclusively a spin singlet electronic ground state, and therefore relativistic corrections can be neglected. We assume that for the considered regime of field strengths perturbation theory holds for the description of the interaction of the field with the electronic structure, whereas a nonperturbative treatment is indispensable for the corresponding nuclear dynamics. In addition, we take into account the interaction of the field with the molecule via its dipole moment and polarizability, thereby neglecting higher order contributions due to (higher) hyperpolarizabilities. Thus, in the framework of the Born-Oppenheimer approximation the rovibrational Hamiltonian reads

$$H = T_R + \frac{\hbar^2 \mathbf{J}^2(\theta, \phi)}{2\mu R^2} + V(R) - FD(R) \cos \theta - \frac{F^2}{2} [\alpha_{\perp}(R) \sin^2 \theta + \alpha_{\parallel}(R) \cos^2 \theta], \quad (1)$$

where  $R$  and  $\theta, \phi$  are the internuclear distance and the Euler angles, respectively, and we use the molecule fixed frame with the coordinate origin at the center of mass of the nuclei.  $T_R$  is the vibrational kinetic energy,  $\hbar \mathbf{J}(\theta, \phi)$  is the orbital angular momentum,  $\mu$  is the reduced mass of the nuclei, and  $V(R)$  is the field-free electronic potential energy curve (PEC). The electric field is taken oriented along the  $z$ -axis of the laboratory frame with strength  $F$ . The last three terms provide the interaction between the electric field and the molecule via its permanent electronic dipole moment function (EDMF)  $D(R)$ , and its polarizability, with  $\alpha_{\parallel}(R)$  and  $\alpha_{\perp}(R)$  being the polarizability components parallel and perpendicular to the molecular axis, respectively.

In the presence of the electric field, the dissociation threshold changes and it is given by the quadratic Stark shift of the free atoms, i.e.,  $E_{DT}(F) = -0.5 * F^2(\alpha_1 + \alpha_2)$ , with  $\alpha_i$   $i = 1, 2$  being the polarizabilities of the free atoms. In the presence of the electric field, only the azimuthal symmetry of the molecular wavefunction holds and therefore the magnetic quantum number  $M$  is retained. In this work we focus on levels with vanishing magnetic quantum number  $M = 0$ . For reasons of addressability, we will label the electrically-dressed states by means of their field-free vibrational and rotational quantum numbers  $(\nu, J)$ .

Let us briefly investigate under which conditions the contribution of the molecular polarizabilities can be neglected in the Hamiltonian (1). For simplicity reasons, and without loss of generality, we use the effective rotor approach [37], assuming that the rotational and vibrational energy scales differ significantly and can therefore be separated adiabatically, and that the field influence on the vibrational motion is very small and can consequently be treated by perturbation theory. Then, in the framework of this approximation the rovibrational Hamiltonian (1) is reduced to

$$H_{\nu}^{ERA} = B_{\nu} \mathbf{J}^2 - F \langle D \rangle_{\nu}^0 \cos \theta - \frac{F^2}{2} [\langle \alpha_{\perp} \rangle_{\nu}^0 + \langle \Delta \alpha \rangle_{\nu}^0 \cos^2 \theta] + E_{\nu 00}^0, \quad (2)$$

where  $B_{\nu} = \frac{\hbar^2}{2\mu} \langle R^{-2} \rangle_{\nu}^0$  is the field-free rotational constant of the state with quantum numbers  $\nu$ ,  $J = 0$  and  $M = 0$ ,  $\psi_{\nu 00}^0(R)$  and  $E_{\nu 00}^{(0)}$  are the vibrational wave function and energy, respectively, and we encounter the expectation values

$\langle R^{-2} \rangle_\nu^0 = \langle \psi_{\nu 00}^0 | R^{-2} | \psi_{\nu 00}^0 \rangle$ ,  $\langle D \rangle_\nu^0 = \langle \psi_{\nu 00}^0 | D(R) | \psi_{\nu 00}^0 \rangle$ ,  $\langle \alpha_\perp \rangle_\nu^0 = \langle \psi_{\nu 00}^0 | \alpha_\perp(R) | \psi_{\nu 00}^0 \rangle$ , and  $\langle \Delta\alpha \rangle_\nu^0 = \langle \psi_{\nu 00}^0 | \alpha_\parallel(R) - \alpha_\perp(R) | \psi_{\nu 00}^0 \rangle$ . Within this approach, at a certain field strength  $F$  the interaction due to the polarizability can be neglected in the effective rotor Hamiltonian (2) if  $\left| \frac{2\langle D \rangle_\nu^0}{F\langle \alpha_\perp \rangle_\nu^0} \right| \gg 1$  and  $\left| \frac{2\langle D \rangle_\nu^0}{F\langle \Delta\alpha \rangle_\nu^0} \right| \gg 1$ .

To analyze the very weak field regime, we rescale the effective rotor Hamiltonian (2) with  $B_\nu$ , and assume that the ratios  $\frac{F}{B_\nu}\langle D \rangle_\nu^0$ ,  $\frac{F^2}{2B_\nu}\langle \alpha_\perp \rangle_\nu^0$ , and  $\frac{F^2}{2B_\nu}\langle \Delta\alpha \rangle_\nu^0$  are smaller than the rescaled field-free rotational kinetic energy  $J(J+1)$ . Then, for a certain state with quantum numbers  $\nu$ ,  $J$  and  $M$ , time-independent perturbation theory provides the following second order correction to the field-free energy

$$E_{\nu,J,M}^{(2)} = \left[ A_{JM} \frac{(\langle D \rangle_\nu^0)^2}{B_\nu} - \frac{1}{2} \langle \alpha_\perp \rangle_\nu^0 - \frac{1}{2} \langle \Delta\alpha \rangle_\nu^0 C_{JM} \right] F^2, \quad (3)$$

where the angular coefficients [38] are given by

$$\begin{aligned} A_{JM} &= \frac{J(J+1) - 3M^2}{2J(J+1)(2J+1)(2J+3)} \quad \text{for } J > 0 \\ A_{00} &= -\frac{1}{6} \end{aligned} \quad (4)$$

and

$$C_{JM} = \frac{(J+1)^2 - M^2}{(2J+1)(2J+3)} + \frac{J^2 - M^2}{(2J+1)(2J-1)}. \quad (5)$$

This second order correction to the rotational energy depends on the molecular system and the symmetry of the considered state through the expectation values  $\langle D \rangle_\nu^0$ ,  $\langle \alpha_\perp \rangle_\nu^0$  and  $\langle \Delta\alpha \rangle_\nu^0$ . In the perturbative regime, the polarizability terms can be neglected if  $\left| \frac{2(\langle D \rangle_\nu^0)^2 A_{JM}}{B_\nu \langle \alpha_\perp \rangle_\nu^0} \right| \gg 1$  and  $\left| \frac{2(\langle D \rangle_\nu^0)^2 A_{JM}}{B_\nu \langle \Delta\alpha \rangle_\nu^0 C_{JM}} \right| \gg 1$ . We have  $C_{JM} > |A_{JM}|$ , and the coefficient  $|A_{JM}|$  becomes increasingly smaller than  $C_{JM}$  for increasing values of  $J$ ; for example for  $J = 15$  and  $M = 0$   $A_{15,0} = 4.888 \times 10^{-4}$  and  $C_{15,0} = 0.5005$ , and for  $J = M = 15$   $A_{15,15} = -8.859 \times 10^{-4}$  and  $C_{15,15} = 3.030 \times 10^{-2}$ . As a consequence we encounter the situation that for high rotational excitations of certain molecular systems the interaction due to the molecular polarizability could be the dominant one. We emphasize that the above considerations are valid only for weak fields and within the effective rotor approach.

### III. RESULTS

In the present work, we have performed a full rovibrational study of the influence of an external static electric field on the highly excited rovibrational states of the LiCs molecule. The PEC, EDMF and polarizability components of the  $^1\Sigma^+$  electronic ground state of LiCs are plotted as a function of the internuclear distance in Figures 1(a), and (b), respectively. For the PEC, we use the experimental data of ref.[39], which includes for the long-range behaviour the van der Waals terms,  $-\sum_{n=6,8,10} C_n/R^n$ , and an exchange energy term,  $-AR^\gamma e^{-\beta R}$ , see ref.[39] for the values of these parameters. The EDMF and polarizabilities are taken from semi-empirical calculations performed by the group of Dulieu [32, 40]. The EDMF is negative and its minimum is shifted by  $1.4 a_0$  with respect to the equilibrium internuclear distance  $R_e = 6.94 a_0$  of the PEC. For the electronic ground state of the polar alkali dimers the long-range behaviour of the EDMF is given by  $D_7/R^7$  [41], this function has been fitted to the theoretical data for  $R \gtrsim 18.15 a_0$  with  $D_7 = -5 \times 10^{-6}$  a.u. Regarding the polarizability, both components smoothly change as  $R$  is enhanced and  $\alpha_\perp(R) \geq \alpha_\parallel(R)$  for any  $R$  value. They satisfy that  $\lim_{R \rightarrow \infty} \alpha_\perp(R) = \lim_{R \rightarrow \infty} \alpha_\parallel(R) = \alpha_{Li} + \alpha_{Cs}$ , with the polarizabilities of the Li and Cs atoms  $\alpha_{Li} = 164.2$  a.u. and  $\alpha_{Cs} = 401$  a.u., respectively, [42, 43]. Thus, for  $R \gtrsim 26 a_0$  the theoretical data were extrapolated by means of exponentially decreasing functions to match the constant value  $\alpha_{Li} + \alpha_{Cs}$ . For computational reasons,  $\alpha_\perp(R)$  and  $\alpha_\parallel(R)$  are extrapolated for  $R < 5$  and  $4 a_0$ , respectively. Since this study is focused on highly excited levels lying close to the dissociation threshold, we are aware of the fact that our results strongly depend on the assumptions made for the long-range behaviour of  $D(R)$ ,  $\alpha_\perp(R)$  and  $\alpha_\parallel(R)$ , and on the extrapolations performed at short-range for  $\alpha_\perp(R)$  and  $\alpha_\parallel(R)$ . However, let us remark that the overall behaviour and physical phenomena presented here remain unaltered as these parameters are altered.

For the lowest rotational excitations within each vibrational band of LiCs, we have investigated and compared the field interactions with the dipole moment and polarizability presented in the previous section. Within perturbation theory, the interaction due to the molecular polarizability becomes comparable to the one due to the dipole moment only for the last two vibrational bands. Assuming that the effective rotor conditions are satisfied, the interaction with

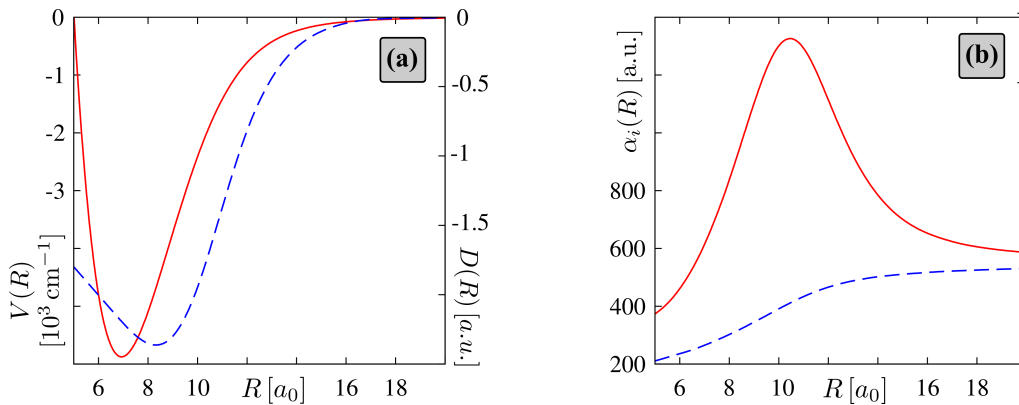


FIG. 1: (a): Electronic potential curve (solid) and electric dipole moment functions (dashed), and (b): parallel  $\alpha_{\parallel}(R)$  (solid) and perpendicular  $\alpha_{\perp}(R)$  (dashed) components of the polarizability of the electronic ground state of the LiCs molecule.

the polarizability can be neglected for those levels with  $\nu \leq 47$  and  $48 \leq \nu \leq 52$  if the field strength is smaller than  $10^{-3}$  and  $2 \times 10^{-4}$  a.u., respectively. Whereas, for the vibrational bands  $\nu = 53$  and  $54$  both interactions possess the same order of magnitude for the much weaker fields  $F \approx 6 \times 10^{-5}$  and  $8 \times 10^{-6}$  a.u., respectively. Furthermore, the absolute values of the quadratic Stark shifts of the atomic energies are larger than the binding energies of the last bound state for  $F \gtrsim 10^{-5}$  a.u., which also justifies that the interaction with the polarizability has to be included in the present study.

Here, we consider the highest rotational excitations ( $M = 0$ ) for the last four vibrational bands,  $51 \leq \nu \leq 54$ , of LiCs with binding energies smaller than  $0.28 \text{ cm}^{-1}$ . We focus on the strong field regime  $F = 10^{-6} - 3.4 \times 10^{-4}$  a.u., i.e.,  $F = 5.14 - 1747.6 \text{ kV/cm}$ , which includes the experimentally accessible range of strong static fields and possibly quasistatic fields. We remark that such strong fields are considered to induce the below-described peculiar behaviour of these states. Most of the overall probability is located at the outermost hump of these states, i.e., in regions where the EDMF possesses small values and the polarizabilities are close to  $\alpha_{Li} + \alpha_{Cs}$ . Thus, strong fields are needed in order to observe a significant field-effect on these levels. At these field strengths the corresponding rovibrational dynamics cannot be described by means of the effective or (due to avoided crossings) even the adiabatic rotor approximations [37, 44], and, of course not by perturbation theory (3). Hence, the two-dimensional Schrödinger equation associated to the nuclear Hamiltonian (1) has to be solved numerically. We do this by employing a hybrid computational method which combines discrete and basis-set techniques applied to the radial and angular coordinates, respectively [13, 37].

Since in the presence of the field the dissociation threshold is  $E_{DT}(F) = -0.5 * F^2(\alpha_{Li} + \alpha_{Cs})$ , we define the energetical shift with respect to this dissociation threshold as  $\varepsilon_{\nu,J} = E_{\nu,J}(F) - E_{DT}(F)$ , with  $E_{\nu,J}(F)$  being the energy of the  $(\nu, J)$  state at field strength  $F$ . Figure 2(a) shows these Stark shifts  $\varepsilon_{\nu,J}$  satisfying  $\varepsilon_{\nu,J} \geq -0.28 \text{ cm}^{-1}$  in the above-provided range of field strengths. This spectral window includes the  $(54, 0)$ ,  $(54, 1)$ ,  $(53, 4)$ ,  $(53, 5)$ ,  $(53, 6)$ ,  $(52, 10)$  and  $(51, 15)$  states, and for  $F \gtrsim 3 \times 10^{-4}$  a.u. also the  $(52, 9)$  level. Since all these levels possess the same symmetry ( $M = 0$ ) for  $F \neq 0$ , and since the field strength is the only parameter at hand to vary the rovibrational energies, the von Neumann-Wigner noncrossing rule [45] holds and we encounter only avoided crossings of energetically adjacent states but no exact crossings in the field-dressed spectrum. In the vicinity of the avoided crossing the nuclear dynamics is dominated by a strong interaction and mixing of the involved rovibrational states. For reasons of simplicity (according to the Landau-Zener theory) we assume that the avoided crossings are traversed diabatically as  $F$  is increased. Thus, a certain state has the same character before and after the avoided crossing, e.g. taking for example the  $(54, 0)$  level we observe that it keeps its high-field seeking trend, see Figure 2(a).

Before studying these avoided crossings in more detail, let us analyze the general behaviour of the binding energies. For all  $\varepsilon_{\nu,J}$  we observe a very weak dependence on  $F$  for  $F \lesssim 3 \times 10^{-5}$  a.u. The larger the field-free rotational quantum number of a state, the stronger is the field strength needed to encounter a deviation of  $\varepsilon_{\nu,J}$  from its field-free value. With a further enhancement of the strength,  $\varepsilon_{\nu,J}$  increases (decreases) for the high (low)-field seekers. The strong field dynamics is dominated by pendular states, whose binding energies increase as  $F$  is augmented. Their main feature is their orientation along the field axis: They represent coherent superpositions of field-free rotational levels [38]. In our spectral region, this regime is only reached for the  $(54, 0)$ ,  $(54, 1)$  and  $(53, 4)$  states. Indeed,  $\varepsilon_{54,0}$  monotonically decreases as  $F$  increase, whereas  $\varepsilon_{54,1}$  and  $\varepsilon_{53,4}$  initially increase and reach broad maxima, decreasing thereafter. In contrast, the binding energies of the  $(52, 9)$ ,  $(52, 10)$ ,  $(53, 6)$  and  $(53, 5)$  decrease as  $F$  is increased. Due to its large field-free angular momentum, the  $(51, 15)$  level is the least affected by the field. Initially,  $\varepsilon_{51,15}$  is reduced as  $F$  is enhanced, passes through a broad minimum and increases thereafter. The contribution of the molecular polarizability

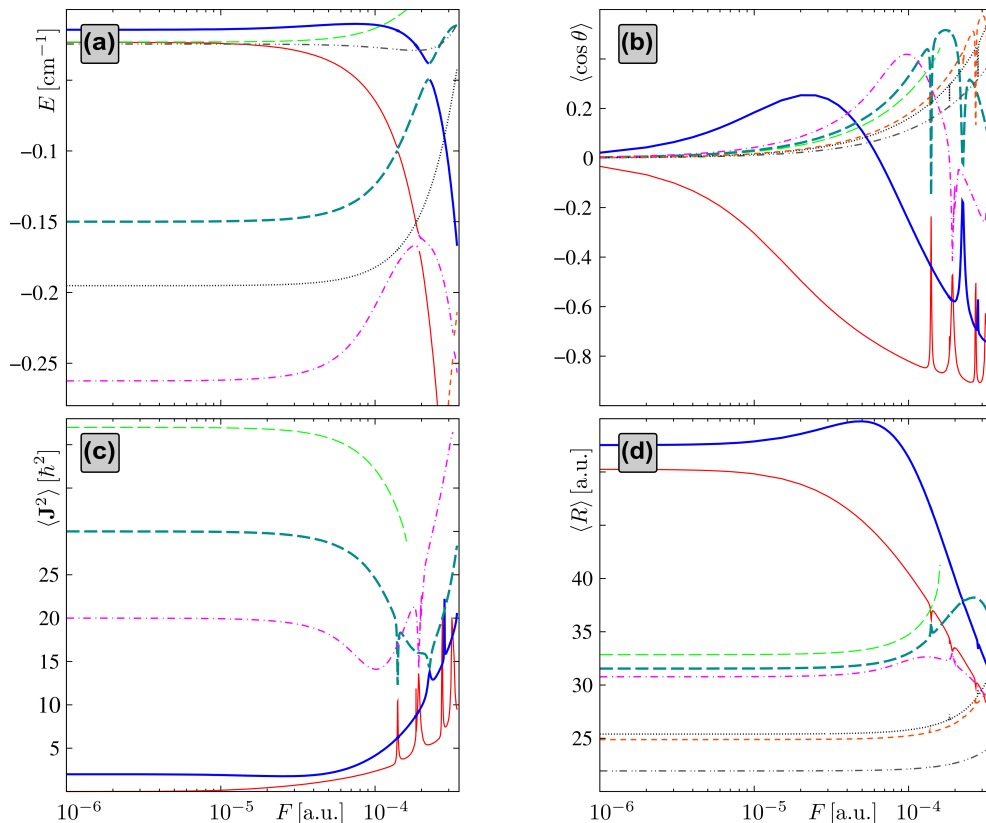


FIG. 2: (a) Energy shifts with respect to the dissociation threshold  $\varepsilon_{\nu J}$ , and expectation values (b)  $\langle \cos \theta \rangle$ , (c)  $\langle \mathbf{J}^2 \rangle$  and (d)  $\langle R \rangle$ , as a function of the field strength for the states with field-free vibrational and rotational quantum numbers (54, 0) (solid), (54, 1) (solid thick), (53, 4) (dotted-dashed), (53, 5) (long dashed thick), (53, 6) (long dashed), (52, 10) (dotted), (52, 9) (short dashed), and (51, 15) (double dotted-dashed). Note that in the panel (c) only the results for the levels (54, 0), (54, 1), (53, 4), (53, 5) and (53, 6) are included.

causes that this state is a high-field seeker in the weak field regime, whereas if only the interaction with the dipole moment is included it has a low-field seeking character.

Regarding the avoided crossings, some of them are very narrow and can not be identified as such on the scale used in Figure 2(a), e.g. those among the pairs of levels (54, 1) – (53, 6), (54, 1) – (51, 15), (54, 0) – (51, 15), and (54, 0) – (52, 10). In contrast, other avoided crossings are very broad, and they are characterized by a strong coupling between the involved molecular states. The avoided crossing between the (54, 1) and (53, 5) levels takes places at strong fields, and the minimal energetical gap is  $\Delta E = |\varepsilon_{54,1} - \varepsilon_{53,5}| = 1.13 \times 10^{-2} \text{ cm}^{-1}$  for  $F \approx 2.23 \times 10^{-4} \text{ a.u.}$  The (54, 0) state is involved in an avoided crossing with the (53, 5) level characterized by  $\Delta E = |\varepsilon_{54,0} - \varepsilon_{53,5}| = 2.82 \times 10^{-3} \text{ cm}^{-1}$  for  $F \approx 1.399 \times 10^{-4} \text{ a.u.}$ , and another one with the (53, 4) state with  $\Delta E = |\varepsilon_{54,0} - \varepsilon_{53,4}| = 1.08 \times 10^{-2} \text{ cm}^{-1}$  for  $F \approx 1.918 \times 10^{-4} \text{ a.u.}$  The (53, 4) level experiences an avoided crossing with the (52, 9) state, with minimal energetical separation  $\Delta E = |\varepsilon_{53,4} - \varepsilon_{52,9}| = 1.12 \times 10^{-2} \text{ cm}^{-1}$  for  $F \approx 3.25 \times 10^{-4} \text{ a.u.}$  For other alkali dimers weaker electric field strengths might suffice to exhibit similar avoided crossings. These avoided crossings are wide enough to be experimentally observed in a similar way as it has been done for the weakly bound spectrum of  $\text{Cs}_2$  dimer in a magnetic field [46]. In this system coupling strengths,  $\frac{\Delta E}{2}$ , larger than  $1.67 \times 10^{-6} \text{ cm}^{-1}$  were experimentally estimated; i.e., even the energetical separation of the (54, 1) and (53, 6) avoided crossing,  $\Delta E = |\varepsilon_{54,1} - \varepsilon_{53,6}| = 9.6 \times 10^{-5} \text{ cm}^{-1}$  for  $F \approx 1.1 \times 10^{-4} \text{ a.u.}$ , could be measured. Moreover, as it has been done for the  $\text{Cs}_2$  molecule [36, 46] in a magnetic field, a suitable electric-field ramp could be used to transfer population from high to low rotational excitations in a controlled way, by either diabatically jumping or adiabatically following these electrically induced avoided crossings.

An interesting physical phenomenon is observed in the evolution of the (53, 6) level in the spectrum.  $\varepsilon_{53,6}$  increases as  $F$  increases, and after passing the avoided crossing with the (54, 1),  $\varepsilon_{53,6}$  becomes positive for  $F \gtrsim 1.6 \times 10^{-4} \text{ a.u.}$  The Stark increase of the (53, 6) energy surpasses the reduction of the dissociation threshold, and this level is shifted to the continuum. Hence, if the LiCs is initially in the (53, 6) level, it will dissociate as the field strength is adiabatically tuned and enhanced above  $F \gtrsim 1.6 \times 10^{-4} \text{ a.u.}$  Therefore a channel for molecular dissociation is opened as the electric field is modified. Of course, the inverse process is also possible, and the continuum state formed by two free atoms can

be brought into a bound state by lowering the electric field strength. Indeed, it has been proved that a static electric field could be used to manipulate the interaction between two atoms such that a virtual state could be transformed in a new bound state, i.e., the molecular system supports a new bound level [23].

To illustrate the appearance of this phenomenon for a low-lying rotational excitation, we have performed a similar study for a designed molecule. We have taken the theoretical PEC of the  $^1\Sigma^+$  electronic ground state of LiCs computed by the group of Allouche [47] with the van der Waals long-range potential,  $C_6/R^6$ , but modifying the LiCs  $C_6$  coefficient to  $C_6 = 2225$  a.u. The (54, 1) level is shifted towards the dissociation threshold, having a field-free energy  $E_{54,1} \approx -5.9 \times 10^{-5}$  cm $^{-1}$ . As electric dipole moment function and polarizabilities we have used the corresponding functions of the LiCs molecule described above. The last most weakly bound states of this toy system have been studied in the presence of a static electric field, but for the sake of simplicity we discuss here only the results for the (54, 1) level. As  $F$  is enhanced  $\varepsilon_{54,1}$  increases, and becomes positive for  $F \gtrsim 5 \times 10^{-5}$  a.u.; note that this field strength is much weaker than the above used ones. For a bound level, a further enhancement of the field would change its character, and its binding energy would increase as  $F$  is augmented. We have observed the same phenomenon for the (54, 1) state, which becomes bound again for  $F \gtrsim 1.7 \times 10^{-4}$  a.u., and  $\varepsilon_{54,1}$  decreases thereafter. The level has been captured by the nuclear potential demonstrating that the reverse process is possible. Starting with two free atoms with the correct internal symmetry, by adiabatically tuning the field the dimer is formed in a highly excited level.

Due to negative sign of the EDMF, the main feature of the pendular regime (focusing again on LiCs) is the antiparallel orientation of the states along the field axis. The orientation can be estimated by the expectation value  $\langle \cos \theta \rangle$ : The closer  $|\langle \cos \theta \rangle|$  is to one, the stronger is the orientation of the state along the field. Figure 2(b) illustrates the evolution of  $\langle \cos \theta \rangle$  as the field strength is changing. The initial behaviour of  $\langle \cos \theta \rangle$  for weak fields depends on the character of the corresponding level. For the (54, 0) state  $\langle \cos \theta \rangle$  monotonically decreases as  $F$  is increased, it achieves the largest orientation with  $\langle \cos \theta \rangle \leq -0.7$  for  $F \gtrsim 5 \times 10^{-5}$  a.u., except in the proximity of avoided crossings. For the (54, 1), (53, 5) and (53, 4) levels,  $\langle \cos \theta \rangle$  reach a broad maximum decreasing thereafter. The orientation of the (54, 1) and (53, 4) states becomes antiparallel for stronger fields. Not considering the proximity of an avoided crossing region, the (54, 1) state shows a significant orientation with  $\langle \cos \theta \rangle \leq -0.4$  for  $F \gtrsim 1.31 \times 10^{-4}$  a.u. The remainder of states keep a pinwheeling character, and  $\langle \cos \theta \rangle$  increases as  $F$  is augmented. Since we have used the notation that the avoided crossings are traversed diabatically, a certain state  $\langle \cos \theta \rangle$  reestablishes its increasing or decreasing trend once the avoided crossing has been passed. The smooth behaviour of  $\langle \cos \theta \rangle$  is significantly distorted by the presence of these spectral features, where due to the strong mixing and interaction among the two involved states  $\langle \cos \theta \rangle$  exhibits sharp and pronounced maxima and minima. For example, the avoided crossing among the (54, 0) and (53, 5) levels, is characterized by the values  $\langle \cos \theta \rangle_{54,0} = -0.235$  and  $\langle \cos \theta \rangle_{53,5} = -0.152$ , for  $F = 1.399 \times 10^{-4}$  a.u., compared to the results  $\langle \cos \theta \rangle_{54,0} = -0.847$  and  $\langle \cos \theta \rangle_{53,5} = 0.436$  obtained for  $F = 1.3 \times 10^{-4}$  a.u. Note that for the (54, 0) level  $\langle \cos \theta \rangle$  shows an additional maximum for  $F \gtrsim 3 \times 10^{-4}$ , i.e., this level suffers another avoided crossing which is not observed in Figure 2(a), because  $\varepsilon_{54,0} < -0.28$  cm $^{-1}$  for  $F \geq 2.54 \times 10^{-4}$  a.u.

The expectation value  $\langle \mathbf{J}^2 \rangle$  of the states (54, 0), (54, 1), (53, 4), (53, 5) and (53, 6), is presented as a function of the electric field in Figure 2(c). To provide a reasonable scale, the results for the (52, 10), (52, 9) and (51, 15) levels have not been included. This quantity provides a measure for the mixture of field-free states with different rotational quantum numbers  $J$  but the same value for  $M$ , i.e., it describes the hybridization of the field-free rotational motion. Analogous to the binding energy,  $\langle \mathbf{J}^2 \rangle$  shows for weak fields a plateau-like behaviour: The hybridization of the angular motion is very small and the dynamics is dominated by the field-free rotational quantum number of the corresponding state. For stronger fields, these states possess a rich rotational dynamics, with significant contributions of different partial waves, and  $\langle \mathbf{J}^2 \rangle$  decreases (increases) for the low-(high)-field seekers as  $F$  is enhanced. In the strong field regime,  $\langle \mathbf{J}^2 \rangle$  shows a broad minimum for the (54, 1), (53, 4) and (53, 5) states, increasing thereafter. The pendular limit is characterized by the augment of  $\langle \mathbf{J}^2 \rangle$  due to the contribution of higher field-free rotational states. This regime is only achieved by the (54, 0), (54, 1) and (53, 4) levels. In contrast, the mixing with lower rotational excitations is dominant for the (53, 5) and (53, 6) states, and  $\langle \mathbf{J}^2 \rangle \leq J(J+1)$ , with  $J$  being the corresponding field-free rotational quantum number; similar results are obtained for the (52, 9), (52, 10) and (51, 15) states not included in Figure 2(c). The presence of the avoided crossings significantly distorts the smooth behaviour of  $\langle \mathbf{J}^2 \rangle$ . The  $\langle \mathbf{J}^2 \rangle$  of the level in an avoided crossing with the lowest (highest) field-free  $J$  exhibits a pronounced and narrow maximum (minimum) on these irregular regions. At the smallest energetical gap, we encounter similar values of  $\langle \mathbf{J}^2 \rangle$  for both states. For example, for  $F = 1.399 \times 10^{-4}$  a.u. we obtain  $\langle \mathbf{J}^2 \rangle = 10.38 \hbar^2$  and  $12.40 \hbar^2$  for the (54, 0) and (53, 5) levels, respectively, compared to the values  $\langle \mathbf{J}^2 \rangle_{54,0} = 3.04 \hbar^2$  and  $\langle \mathbf{J}^2 \rangle_{53,5} = 20.75 \hbar^2$  for  $F = 1.3 \times 10^{-4}$  a.u.

The expectation value of the radial coordinate  $\langle R \rangle$  is presented for these states and range of field strengths in Figure 2(d). Only if the vibrational motion is affected by the field  $\langle R \rangle$  should differ from its field-free value. Analogously to  $\varepsilon_{JM}$  and  $\langle \mathbf{J}^2 \rangle$ ,  $\langle R \rangle$  represents approximately a constant for weak fields, and strong fields are needed to observe significant deviations from its field-free value. Indeed, the larger is the rotational quantum number of a state for  $F = 0$ , the least affected by the field is its  $\langle R \rangle$ . For the (54, 0) level,  $\langle R \rangle$  monotonically decreases from  $50.24 a_0$  to  $28.13 a_0$  as  $F$  is enhanced from 0 to  $3.4 \times 10^{-4}$  a.u. For the (54, 1), (53, 5) and (53, 4) states,  $\langle R \rangle$  increases as

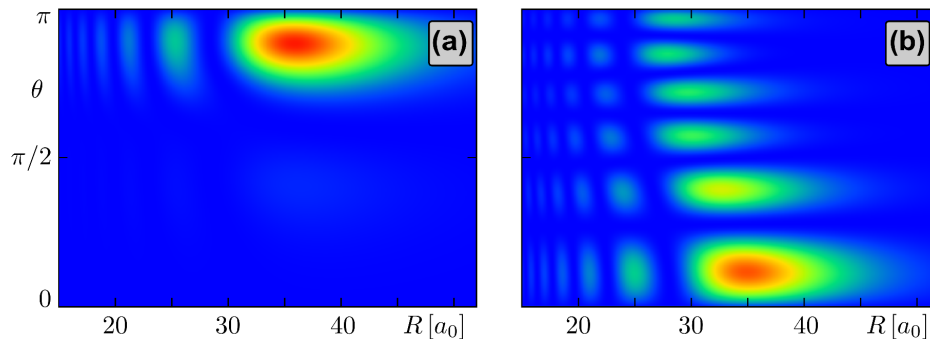


FIG. 3: Probability densities (a) of the state (54, 0) and (b) of the state (53, 5) for  $F = 1.3 \times 10^{-4}$  a.u., i.e., close to the avoided crossing but still without mixing of the rovibrational field-dressed states.

$F$  is augmented, reaches a broad maximum and decreases thereafter. The (54, 1) level is significantly affected with a reduction from  $\langle R \rangle = 52.52 a_0$  to  $30.96 a_0$  for  $F = 0$  and  $3.4 \times 10^{-4}$  a.u., respectively. For the (53, 4) state this effect is much smaller, and  $\langle R \rangle$  is modified from the field-free result  $30.78 a_0$  to  $28.32 a_0$ . For (53, 5) we observe that for  $F = 3.4 \times 10^{-4}$  a.u.  $\langle R \rangle$  is by  $4.57 a_0$  larger than its value for  $F = 0$ .  $\langle R \rangle$  increases as  $F$  is enhanced for the remaining states, their total rise being smaller than  $5 a_0$  for the analyzed levels  $\nu = 51$  and  $52$ . As the (53, 6) state is shifted to the continuum, the slope of  $\langle R \rangle$  becomes very steep, and  $\langle R \rangle$  is enhanced from  $\langle R \rangle = 32.85 a_0$  up to  $41.30 a_0$  for  $F = 0$  and  $1.6 \times 10^{-4}$  a.u., respectively. The field effect on the vibrational motion can be explained as follows: The probability density of those levels with a antiparallel (parallel) orientation is mostly located in the  $\pi/2 \leq \theta \leq \pi$  ( $0 \leq \theta \leq \pi/2$ ) region, where the dipole moment interaction is attractive (repulsive). As a consequence, the wavefunctions are squeezed (stretched) compared to their field-free counterparts to reduce the energy. Again, in the vicinity of the avoided crossing  $\langle R \rangle$  exhibits very similar values for the two involved states. For example, we have found that  $\langle R \rangle = 33.02$  and  $33.13 a_0$  for the states (54, 0) and (53, 5) and  $F = 1.399 \times 10^{-4}$  a.u., respectively.

To gain a deeper insight into the coupling of the vibrational and rotational motions induced by the electric field, we have analyzed the corresponding wavefunctions of two states involved in an avoided crossing. As an example, we discuss here the (54, 0)-(53, 5) avoided crossing. For comparison, let us first analyze their wavefunctions for  $F = 1.3 \times 10^{-4}$  a.u., i.e., 'below' the avoided crossing where the mixing is not yet appreciable. The contour plots of the probability densities,  $|\psi(R, \theta)|^2 \sin \theta$ , in the  $(R, \theta)$  plane are presented in Figures 3(a) and (b) for the (54, 0) and (53, 5) states, respectively. Since most of the overall probability of these weakly bound levels is located in the outer most hump, the radial coordinate has been restricted in these plots to the interval  $15 a_0 \leq R \leq 52 a_0$ . Indeed, more than 89% of the (54, 0) and (53, 5) probability densities are located for  $R > 30 a_0$ , and  $25 a_0$ , respectively. Due to the pronounced antiparallel orientation of the (54, 0) level,  $\langle \cos \theta \rangle = -0.847$ , the corresponding probability density shows a pendular-like structure, it is located in the region  $3\pi/4 \leq \theta \leq \pi$  and the maximal value is obtained at  $\theta = 2.77$  and  $R = 35.87 a_0$ . The typical oscillator-like behaviour with 6 maxima reminiscent from its field free angular momentum  $J = 5$  is observed in the (53, 5) probability density, see Figure 3(b). Since this state has still a pinwheeling character, the corresponding probability density is distributed over the complete interval  $0 \leq \theta \leq \pi$ , however, due to the parallel orientation of this state,  $\langle \cos \theta \rangle = 0.437$ , the probability density is larger in the region  $\theta \leq \pi/2$ . Moreover, the influence of the field on the vibrational motion provokes an inclination of the internuclear axis of this level, i.e., the corresponding wavefunction is stretched and squeezed in the regions  $\theta < \pi/2$  and  $\theta > \pi/2$ , respectively. The squeezing effect also appears for the (54, 0) state which possesses a strong antiparallel orientation (see Figure 3(a)).

As the electric field is enhanced approaching the region of the avoided crossing, a strong interaction between the involved states takes places and the rovibrational dynamics is affected drastically. The contour plots of the (54, 0) and (53, 5) states for  $F = 1.399 \times 10^{-4}$  a.u., which corresponds with the minimal energetical gap between them, are shown in Figures 4(a) and (b), respectively. Although, at this field strength their orientation and hybridization of the angular motion are very similar, there exist significant differences with respect to their wavefunctions. The above-described regular structures typical for an oscillator and pendular-like distributions are lost. Even more, for both levels it is not possible to identify an orientation of the molecule, and the most pronounced maxima are not necessarily located at the outermost turning points. The (54, 0) probability density is distributed in the interval  $0 \leq \theta \leq \pi$ , the largest maximum is at  $\theta = 2.701$  and  $R = 34.02 a_0$ , and it is accompanied by several less pronounced maxima at smaller  $\theta$  values. The (53, 5) probability density exhibits three maxima with similar probability density, the first one at  $\theta = 0.44$  and  $R = 35.24 a_0$ , the second one at  $\theta = 2.95$  and  $R = 33.73 a_0$ , and the third one, at  $\theta = 2.70$  and  $R = 25.97 a_0$ , which is shifted towards smaller internuclear separations from the outermost turning point. Both configurations exhibit significantly distorted patterns, and they show a strong mixing between the radial



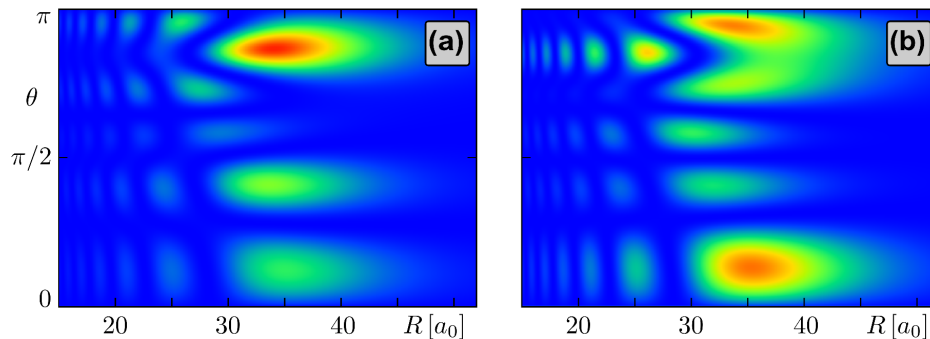


FIG. 4: Probability densities (a) of the state (54, 0) and (b) of the state (53, 5) at the field strength  $F = 1.399 \times 10^{-4}$  a.u.

and angular degrees of freedom. In general, at the avoided crossings the nuclear dynamics of the field-dressed states are characterized by an asymmetric and strongly distorted behavior, exhibiting pronounced localization phenomena.

We have also analyzed these weakly bound levels taking into account only the interaction of the field with the permanent electric dipole, and not considering the contribution of the molecular polarizability. The results look qualitatively similar but show a quantitatively different behaviour as a function of the electric field, and the effect of the polarizability becomes important for  $F \gtrsim 10^{-4}$  a.u. The polarizability terms cause the mixing of states with field-free rotational quantum numbers  $J$  and  $J \pm 2$ . If the polarizability is included, the dissociation energies are smaller, i.e., for a certain  $F$  value the modulus of the displacement of the dissociation threshold is larger than the modulus of the energetical shift due to polarizability of a certain level, and the avoided crossings are also broader. Without the contribution of the polarizability term the (53, 6) level is not shifted to the continuum as the field is increased, and the inverse phenomenon appears, i.e., the (54, 2) level becomes a bound state for  $F \gtrsim 1.8 \cdot 10^{-4}$  a.u.

The validity of the adiabatic and effective rotor approaches has been previously demonstrated for vibrational low-lying levels of the LiCs dimer [33]. However, this does not hold true for the part of the spectrum considered here. Since both approximations do not include the full coupling between the vibrational and rotational motion, the presence of the avoided crossings in the spectrum is not reproduced. In addition, significant errors are found for the binding energies and the expectation value  $\langle R \rangle$  of the rotational excitations even in the absence of the field, e.g. the (53, 6) and (51, 15) levels are not bound within these approaches. The above-discussed field-effects on the vibrational motion can not be explained using an effective rotor description [37]. However, the adiabatic results qualitatively reproduce the orientation and hybridization of the angular motion as well as the stretching and squeezing of the vibrational motion. Numerically significant deviations are encountered in the avoided crossing regions.

#### IV. CONCLUSIONS AND OUTLOOK

We have investigated the influence of a strong static and homogeneous electric field on the highly excited rovibrational states of the electronic ground state  $X^1\Sigma^+$  of the alkali dimer LiCs by solving the fully coupled rovibrational Schrödinger equation. The interaction of the field with the electric dipole moment function as well as with the molecular polarizability has been taken into account. We focus here on the last rotational excitations with vanishing azimuthal symmetry within the last four vibrational bands,  $51 \leq \nu \leq 54$ . Due to their large extension, strong fields are needed in order to observe a significant field influence.

The richness and variety of the resulting field-dressed rotational dynamics has been illustrated by analyzing the energetical Stark shifts, as well as, the orientation, the hybridization of the angular motion and the vibrational stretching and squeezing effects. Whether we encounter a squeezing or stretching of the vibrational motion depends on the angular configuration: The molecule tries to minimize its energy leading to stretching for a parallel configuration and squeezing for an antiparallel one. In the strong field regime, the electrically-dressed spectrum is characterized by the presence of pronounced avoided crossings between energetically adjacent levels. These irregular features lead to a strong field-induced mixing and interaction between the states, and they cause strongly distorted and asymmetric features of the corresponding probability densities. We stress the importance of identifying these irregular features: Their presence affects the radiative decay properties of the dimer, such as lifetime and transition probability for spontaneous decay, and they might significantly alter the chemical reaction dynamics. Even more, one of their possible applications is their use to transfer population between the involved states.

We have demonstrated that if the last most weakly bound state is a low-field seeker it is possible to shift it to the atomic continuum by tuning the electric field, i.e., the molecular system dissociates into free atoms. The reverse process



is also possible, i.e., a continuum state, formed by two free atoms with the correct field-free rotational symmetry, can be transferred to a weakly bound molecular state by changing the field strength. These results suggest that by properly increasing or decreasing the value of the electric field, one could study in a control way the opening of a dissociation or an association channel.

Although our study is restricted to a LiCs dimer and to the spectral region close to the dissociation threshold of its electronic ground state, we stress that the above-observed physical phenomena are expected to occur in many other polar molecules.

### Acknowledgments

Financial support by the Spanish projects FIS2008-02380 (MEC) and FQM-0207, FQM-481 and P06-FQM-01735 (Junta de Andalucía) is gratefully appreciated. This work was partially supported by the National Science Foundation through a grant for the Institute for Theoretical Atomic, Molecular and Optical Physics at Harvard University and Smithsonian Astrophysical Observatory. Financial support by the Heidelberg Graduate School of Fundamental Physics in the framework of a travel grant for R.G.F. is gratefully acknowledged. We thank Michael Mayle for his help with respect to technical aspects of this work.

- 
- [1] K.-K. Ni, S. Ospelkaus, M. H. G. de Miranda, A. Pe'er, B. Neyenhuis, J. J. Zirbel, S. Kotochigova, P. S. Julienne, D. S. Jin, and J. Ye, *Science* **322**, 231 (2008).
  - [2] J. Deiglmayr, A. Grochola, M. Repp, K. Mörtlbauer, C. Glück, J. Lange, O. Dulieu, R. Wester, and M. Weidemüller, *Phys. Rev. Lett.* **101**, 133004 (2008).
  - [3] A. V. Gorshkov, P. Rabl, G. Pupillo, A. Micheli, P. Zoller, M. D. Lukin, and H. P. Büchler, *Phys. Rev. Lett.* **101**, 073201 (2008).
  - [4] C. Ticknor, *Phys. Rev. Lett.* **100**, 133202 (2008).
  - [5] T. V. Tscherbul and R. V. Krems, *J. Chem. Phys.* **125**, 194311 (2006).
  - [6] A. V. Avdeenkov, M. Kajita, and J. L. Bohn, *Phys. Rev. A* **73**, 022707 (2006).
  - [7] R. V. Krems, *Phys. Chem. Chem. Phys.* **10**, 4079 (2008).
  - [8] D. DeMille, *Phys. Rev. Lett.* **88**, 067901 (2002).
  - [9] S. F. Yelin, K. Kirby, and R. Côté, *Phys. Rev. A* **74**, 050301 (2006).
  - [10] A. André, D. DeMille, J. M. Doyle, M. D. Lukin, S. E. Maxwell, P. Rabl, R. J. Schoelkopf, and P. Zoller, *Nat. Phys.* **2**, 636 (2006).
  - [11] P. Pellegrini, M. Gacesa, and R. Côté, *Phys. Rev. Lett.* **101**, 053201 (2008).
  - [12] E. Juarros, P. Pellegrini, K. Kirby, and R. Côté, *Phys. Rev. A* **73**, 041403(R) (2006).
  - [13] R. González-Férez, M. Weidemüller, and P. Schmelcher, *Phys. Rev. A* **76**, 023402 (2007).
  - [14] R. González-Férez, M. Mayle, and P. Schmelcher, *Europhys. Lett.* **78**, 53001 (2007).
  - [15] S. Kotochigova, *Phys. Rev. Lett.* **99**, 073003 (2007).
  - [16] J. Doyle, B. Friedrich, R. V. Krems, and F. Masnou-Seeuws, Special Issue on Ultracold Polar Molecules: Formation and Collisions, *Europhys. J. D* **31** (2004).
  - [17] O. Dulieu, M. Raoult, and E. Tiemann, *J. Phys. B* **39** (2006).
  - [18] W. C. Stwalley and D. Wang, *J. Mol. Spectrosc.* **195**, 194 (1999).
  - [19] K. M. Jones, E. Tiesinga, P. D. Lett, and P. S. Julienne, *Rev. Mod. Phys.* **78**, 483 (2006).
  - [20] T. Köhler, K. Góral, and P. S. Julienne, *Rev. Mod. Phys.* **78**, 1311 (2006).
  - [21] P. O. Fedichev, Y. Kagan, G. V. Shlyapnikov, and J. T. M. Walraven, *Phys. Rev. Lett.* **77**, 2913 (1996).
  - [22] J. L. Bohn and P. S. Julienne, *Phys. Rev. A* **56**, 1486 (1997).
  - [23] M. Marinescu and L. You, *Phys. Rev. Lett.* **81**, 4596 (1998).
  - [24] V. Kokoouline, J. Vala, and R. Kosloff, *J. Chem. Phys.* **114**, 3046 (2001).
  - [25] R. V. Krems, *Phys. Rev. Lett.* **96**, 123202 (2006).
  - [26] Z. Li and R. V. Krems, *Phys. Rev. A* **75**, 032709 (2007).
  - [27] B. Marcelis, B. Verhaar, and S. Kokkelmans, *Phys. Rev. Lett.* **100**, 153201 (2008).
  - [28] F. K. Fatemi, K. M. Jones, and P. D. Lett, *Phys. Rev. Lett.* **85**, 4462 (2000).
  - [29] M. Theis, G. Thalhammer, K. Winkler, M. Hellwig, G. Ruff, R. Grimm, and J. H. Denschlag, *Phys. Rev. Lett.* **93**, 123001 (2004).
  - [30] G. Thalhammer, M. Theis, K. Winkler, R. Grimm, and J. H. Denschlag, *Phys. Rev. A* **71**, 033403 (2005).
  - [31] K. Enomoto, K. Kasa, M. Kitagawa, and Y. Takahashi, *Phys. Rev. Lett.* **101**, 203201 (2008).
  - [32] J. Deiglmayr, M. Aymar, R. Wester, M. Weidemüller, and O. Dulieu, *J. Chem. Phys.* **129**, 064309 (2008).
  - [33] R. González-Férez, M. Mayle, and P. Schmelcher, *Chem. Phys.* **329**, 203 (2006).
  - [34] M. Mayle, R. González-Férez, and P. Schmelcher, *Phys. Rev. A* **75**, 013421 (2007).
  - [35] R. González-Férez, M. Mayle, P. Sánchez-Moreno, and P. Schmelcher, *Europhys. Lett.* **83**, 43001 (2008).

- [36] M. Mark, T. Kraemer, P. Waldburger, J. Herbig, C. Chin, H.-C. Nagerl, and R. Grimm, *Phys. Rev. Lett.* **99**, 113201 (2007).
- [37] R. González-Férez and P. Schmelcher, *Phys. Rev. A* **69**, 023402 (2004).
- [38] K. von Meyenn, *Z. Physik* **231**, 154 (1970).
- [39] P. Staanum, A. Pashov, H. Knockel, and E. Tiemann, *Phys. Rev. A* **75**, 042513 (2007).
- [40] M. Aymar and O. Dulieu, *J. Chem. Phys.* **122**, 204302 (2005).
- [41] W. Byers Brown and D. M. Whisnant, *Chem. Phys. Lett.* **7**, 329 (1970).
- [42] A. Miffre, M. Jacquy, M. Büchner, G. Tréneç, and J. Vigué, *Phys. Rev. A* **73**, 011603 (2006).
- [43] J. M. Amini and H. Gould, *Phys. Rev. Lett.* **91**, 153001 (2003).
- [44] R. González-Férez and P. Schmelcher, *Phys. Rev. A* **71**, 033416 (2005).
- [45] J. V. Neumann and E. Wigner, *Z. Physik* **30**, 467 (1929).
- [46] M. Mark, F. Ferlaino, S. Knoop, J. G. Danzl, T. Kraemer, C. Chin, H.-C. Nagerl, and R. Grimm, *Phys. Rev. A* **76**, 042514 (2007).
- [47] M. Korek, A. Allouche, K. Fakhereddine, and A. Chaalan, *Can. J. Phys.* **78**, 977 (2000).